As per UGC guidelines an electronic bar code is provided to secure your paper

International Journal for Modern Trends in Science and Technology
Volume 12, Issue 05, pages 412-420
ISSN: 2455-3778 online
Available online at: http://www.ijmtst.com/vol12issue05.html
DOI: https://doi.org/10.5281/zenodo.20567847

Frequency Stabilization of Interconnected Power Systems with Hybrid Generation Using TLBO-Optimized PID Control

Dr. J. Srinu Naick | K. Nagamani | D. Usman | Y. Gowtham Yadav | M. Sarath Kumar Reddy

Department of Electrical and Electronics Engineering, Chadalawada Ramanamma Engineering College, Tirupati, Andhra Pradesh, India.

To Cite this Article
Dr. J. Srinu Naick, K. Nagamani, D. Usman, Y. Gowtham Yadav & M. Sarath Kumar Reddy (2026). Frequency Stabilization of Interconnected Power Systems with Hybrid Generation Using TLBO-Optimized PID Control, International Journal for Modern Trends in Science and Technology, 12(05), 412-420. https://doi.org/10.5281/zenodo.20567847

Article Info
Received: 07 May 2026; Revised: 26 May 2026; Accepted: 30 May 2026.

Copyright © The Authors ; This is an open access article distributed under the Creative Commons Attribution License, which permits unrestricted use, distribution, and reproduction in any medium, provided the original work is properly cited.

KEYWORDS

Load Frequency Control (LFC), Automatic Generation Control (AGC), Proportional-Integral-Derivative (PID) Controller, Teaching-Learning-Based Optimization (TLBO), Frequency Stabilization, Interconnected Power Systems, Tie-line Power Deviation, Hybrid Generation Systems, Optimization Techniques, Power System Control

ABSTRACT

: Frequency stabilization in interconnected power systems has become increasingly challenging due to the integration of hybrid generation sources and varying load conditions. Conventional Load Frequency Control (LFC) methods, such as ANN-based coordinated control, utilize energy storage systems and thermal power units to enhance system performance. These approaches employ techniques like Wavelet Packet Decomposition for control signal generation and backpropagation neural networks for disturbance identification. Although effective, such methods suffer from high computational complexity and dependency on training data, limiting their real-time applicability. To address these challenges, this paper proposes a Teaching-Learning-Based Optimization (TLBO) tuned Proportional-Integral-Derivative (PID) controller for Automatic Generation Control (AGC). The proposed controller optimally adjusts its parameters using the TLBO algorithm, which requires fewer tuning parameters and offers faster convergence compared to other metaheuristic techniques. The optimization objective focuses on minimizing frequency deviations and tie-line power fluctuations across interconnected areas. The proposed TLBO-based PID controller is implemented in a multi-area power system incorporating diverse generation sources, including thermal and renewable units. Simulation results demonstrate that the proposed method significantly improves frequency stability, reduces settling time, and enhances overall system performance under varying operating conditions. Hence, the TLBO-optimized PID controller provides a robust and efficient solution for modern power system frequency regulation.

1. Introduction

The reliable operation of interconnected power systems depends on maintaining a continuous balance between power generation and load demand. Any mismatch between generated and consumed power leads to deviations in system frequency, which can adversely affect power quality, equipment performance, and overall system stability [1]. As modern power systems continue to evolve with increasing electricity demand and the integration of renewable energy resources, maintaining frequency stability has become a major challenge for system operators [2]. Consequently, Load Frequency Control (LFC), also known as Automatic Generation Control (AGC), remains one of the most important control functions in interconnected power systems [3]. The primary objective of LFC is to maintain system frequency at its nominal value while regulating tie-line power exchanges between interconnected control areas [4]. In a multi-area power system, sudden load changes in one area can influence the frequency response of neighboring areas through tie-line connections. Therefore, effective frequency control strategies are essential to minimize frequency deviations and maintain scheduled power interchange among interconnected regions [5]. Traditional LFC systems rely on governor, turbine, and generator dynamics to restore frequency following disturbances. However, the increasing complexity of modern power systems has exposed the limitations of conventional control approaches [6]. In recent years, the integration of hybrid generation systems consisting of thermal, hydro, wind, solar photovoltaic (PV), and energy storage units has significantly altered the dynamic behavior of power systems [7]. While renewable energy sources contribute to sustainable power generation and reduced carbon emissions, their intermittent and stochastic nature introduces additional uncertainties into frequency regulation processes [8]. Variations in wind speed and solar irradiance can lead to rapid power fluctuations, resulting in increased frequency oscillations and reduced system inertia [9]. Consequently, maintaining stable frequency in interconnected systems with high renewable penetration requires advanced control techniques capable of handling nonlinearities and uncertainties effectively [10]. Conventionally, Proportional-Integral-Derivative (PID) controllers have been widely employed in AGC applications due to their simple structure, ease of implementation, and satisfactory performance under nominal operating conditions [11]. The proportional component improves transient response, the integral component eliminates steady-state error, and the derivative component enhances damping characteristics. Despite these advantages, fixed-parameter PID controllers often fail to provide optimal performance under varying operating conditions and system parameter uncertainties [12]. Large overshoots, prolonged settling times, and insufficient damping are commonly observed when conventional PID controllers are subjected to significant disturbances or changing system dynamics [13]. To overcome these limitations, researchers have explored various intelligent and adaptive control techniques for frequency regulation. Artificial Neural Networks (ANNs), Fuzzy Logic Controllers (FLCs), and hybrid intelligent controllers have been extensively investigated for AGC applications [14]. ANN-based controllers possess learning and adaptation capabilities that enable them to model nonlinear system behavior and generate effective control actions [15]. For example, ANN-based coordinated control approaches utilize thermal power plants and energy storage systems to enhance frequency regulation performance. Such methods often employ signal-processing techniques such as Wavelet Packet Decomposition (WPD) to generate control signals and backpropagation neural networks for disturbance identification and compensation [16]. Although ANN-based approaches can significantly improve dynamic performance, they are often associated with high computational complexity and extensive training requirements [17]. The accuracy of ANN controllers depends heavily on the availability of representative training datasets and proper network architecture selection. Furthermore, real-time implementation may become challenging due to the computational burden associated with training and updating neural network parameters [18]. These limitations motivate the development of simpler yet effective optimization-based control strategies for practical AGC applications. Metaheuristic optimization techniques have emerged as powerful tools for controller parameter tuning in power system control problems. Algorithms such as Genetic Algorithm (GA), Particle Swarm Optimization (PSO), Differential Evolution (DE), Ant Colony Optimization (ACO), and Artificial Bee Colony (ABC) have been

successfully applied to optimize controller gains and improve frequency regulation performance [19]. These techniques aim to minimize performance indices such as Integral Square Error (ISE), Integral Absolute Error (IAE), and Integral Time Absolute Error (ITAE), thereby reducing frequency deviations and improving system response [20]. Among various optimization methods, the Teaching-Learning-Based Optimization (TLBO) algorithm has attracted considerable attention due to its simplicity, efficiency, and parameter-free nature [21]. Inspired by the teaching and learning process in a classroom, TLBO optimizes solutions through two phases: the teacher phase and the learner phase. Unlike many other metaheuristic algorithms, TLBO does not require algorithm-specific tuning parameters such as crossover probability, mutation rate, or inertia weight, which simplifies implementation and improves convergence characteristics [22]. Moreover, TLBO has demonstrated superior optimization capability and faster convergence in several engineering optimization problems, including power system control applications [23]. The application of TLBO to PID controller tuning offers significant advantages for AGC systems. By optimally determining proportional, integral, and derivative gains, the TLBO algorithm can improve damping performance, reduce overshoot, minimize settling time, and enhance disturbance rejection capability [24]. Such optimized PID controllers retain the simplicity and practicality of conventional PID structures while achieving superior dynamic performance under varying operating conditions. Motivated by these advantages, this paper proposes a TLBO-optimized PID controller for frequency stabilization in interconnected power systems incorporating hybrid generation sources. The proposed controller is employed within the AGC framework to regulate frequency deviations and tie-line power fluctuations across multiple interconnected areas. The TLBO algorithm is utilized to determine optimal PID parameters based on a predefined performance objective function. The effectiveness of the proposed approach is evaluated through simulation studies under different disturbance scenarios and operating conditions. Simulation results demonstrate that the TLBO-optimized PID controller provides faster frequency restoration, reduced oscillations, improved damping characteristics, and better tie-line power regulation compared with conventional control approaches. The proposed method offers a robust, computationally efficient, and practical solution for modern interconnected power systems with high penetration of hybrid generation resources, thereby contributing to enhanced frequency stability and overall system reliability [25].

2. Proposed LFC strategy

2.1. LFC scheme for coordinating energy storage and thermal power

The LFC in a given area should ideally act only on disturbance in that area. Therefore, to avoid frequent operation of the energy storage, the energy storage should only respond to the power imbalance within its area. The proposed LFC strategy in power system with wind power is shown in Fig. 1. As demonstrated in Fig. 1, a back propagation neural network is used to detect disturbance. The output of the neural network is used to indicate whether there is disturbance. If there is disturbance in this area, then path 2 is used, and if not, path 1 is used. In path 2, the energy storage system is used to assist the thermal power plant to improve the speed of responding to the AGC command. Thus, thermal power contributes to the low frequency component of AGC command, energy storage contributes to the high frequency component.

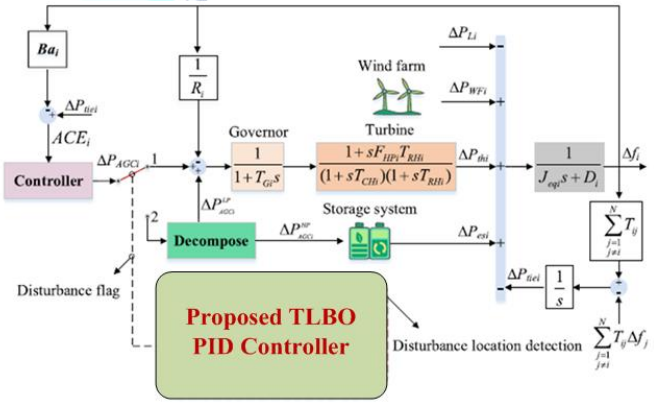

Fig. 1 Proposed method of LFC strategy

2.2. AGC command decomposition

WPD can reflect the non-stationary, short duration, localized characteristics of the time and frequency domain of the signal. Thus, WPD is proposed to decompose AGC commands to coordinate the frequency regulation contribution of thermal and storage, through which the high frequency fluctuation is mitigated by storage system. High and low frequencies are distinguished by the response time of thermal power plants. According to the relationship between the

response time and the frequency domain bandwidth, the frequency domain bandwidth of the output power of the thermal plant can be obtained by:

$$f_{cut} = \frac{0.3}{T_{tht}} \quad (1)$$

Where *f*cut is the bandwidth of thermal plant, and *T*tht is response time. Then, based on this bandwidth, the AGC command can be decomposed into:

$$\Delta P_{AGCi} = \Delta P_{AGCi}^{HF} + \Delta P_{AGCi}^{LF} \quad (2)$$

WPD decomposes the AGC command into components with different center frequencies but the same bandwidth. The relationship between the number of decomposition layers, m, and the bandwidth is

$$f_{cut} \geq \frac{f_s}{2^{m+1}} \quad (3)$$

Here, fs is data sampling frequency, $m \in \mathbb{Z}$. Combining (1) and (3), the minimum number of decomposition layers can be obtained as:

$$m = INT\left(\frac{lgT_{tht} + lgf_s - lg0.35}{lg2}\right) \quad (4)$$

Hence, AGC command decomposes into:

$$\Delta P_{AGCi} = P_0 + \sum_{j=1}^{2^m-1} P_j \quad (5)$$

That is:

$$\Delta P_{AGCi}^{LF} = P_0 \quad (6)$$

$$\Delta P_{AGCi}^{HF} = \sum_{j=1}^{2^m-1} P_j \quad (7)$$

2.3. Energy storage control strategy

In the LFC, the constraints of energy storage must be satisfied. The constraints of energy storage include two aspects: output power and state of charge (SOC). The constrains are:

$$SOC_i(t) = SOC_i(t-1) + \frac{\int_{t-1}^{t}\left(\delta\chi_{ch}P_{esi} - (i-\delta)\frac{P_{esi}}{\chi_{dis}}\right)}{C_{esi}} \quad (8)$$

$$SOC_{mini} \leq SOC_i(t) \leq SOC_{maxi} \quad (9)$$

$$0 \leq P_{esi} \leq P_{es\_max} \quad (10)$$

Where Ces*i* is the nominal capacity of the energy storage, *P*es_max is the nominal power of the energy storage. χch and χdis are the charging efficiency and discharging efficiency, respectively. *SOC*min*i* and *SOC*max*i* are the limits of SOC. δ is binary variable, 1 represents charging, and 0 represents discharging. Energy storage control strategy is an important component of assisting thermal power generation to improve frequency response. To meet the constraints of energy storage, the decomposition layer of WPD obtained by (4) is dynamically adjusted based on the energy storage constrains, as shown in Fig. 2. When the energy storage system is assisting the frequency regulation of the thermal plant, the main concern is the output characteristics. Therefore, the energy storage system is approximated by a first-order inertia element. If the layer number m obtained according to (4) satisfies the energy storage constraint, no adjustment will be made. When the energy storage constraints are not met, if the energy storage power needs to be increased, the number of decomposition layers should be increased, and if the energy storage power needs to be reduced, the number of decomposition layers should be reduced.

2.4. Relationship between controller inverse and ACE

The purpose of LFC is to make the ACE tend to zero. It can be seen from Fig. 1 that the control variable is the output, ΔPAGC*i*, of the controller, and the controlled variable is the *ACEi*. Let the sum of all disturbances be represented by ε, then for area i, the state space model with disturbance as input can be expressed as follows:

$$\dot{\bar{x}}_i = \bar{A}_i\bar{X}_i + \bar{B}_i\varepsilon$$

$$y_i = \bar{c}_i\bar{x}_i \quad (11)$$

Assume the initial value *Xi* (0) =0, then its transfer function is:

$$G_1(s) = \bar{c}_i(s\bar{l} - \bar{A}_i)^{-1}\bar{B}_i \quad (12)$$

At steady state, ACE is equal to zero, so the output power of the steam turbine satisfies:

$$\Delta P_{thi} = -\varepsilon \quad (13)$$

Let the controller be expressed as $H(s)$ in the form of transfer function, and let the transfer function from ΔPAGC*i* to ΔPth*i* path be denoted by $G2(s)$, then, Fig. 1 can be transformed into the equivalent structure diagram as shown in Fig. 5, which is negative feedback. As can be seen from Fig. 5, *ACEi* in the form of transfer function expressed as:

$$ACE_i(s) = \frac{G_1(s)}{1+G_2(s)H(s)G_1(s)}\varepsilon(s) \quad (14)$$

Because

$$\forall\varepsilon, t \to t_s, ACE_i \to 0 \quad (15)$$

Then, there must be at least one pure integral term in $H(s)$ to ensure the steady state value of ACE is zero. The (21) is expanded as follows:

$$ACE_i(s) = \frac{G_2^P(s)H^P(s)G_1^z(s)\varepsilon(s)}{G_2^P(s)H^P(s)G_1^P(s)+G_2^z(s)H^z(s)G_1^z(s)} \quad (16)$$

Where $Gz1(s)$, $Gz2(s)$, $Hz(s)$, $Gp1(s)$, $Gp2(s)$, $Hp(s)$ are numerator and denominator polynomials of the transfer function, respectively. Since there must be at least one pure integral term in $H(s)$ to ensure the steady state value of ACE is zero, so suppose $H(s)$:

$$H(s) = \frac{H^z(s)}{sH_1^P(s)} \quad (17)$$

Let $R(s)$ and $T(s)$ be polynomials of degree $d1$ and $d2$, respectively. if R (s) and $T(s)$ are relatively prime, then there exist polynomials $P(s)$ and Q (s) such that:

$$R(s)P(s) + T(S)Q(s) = L(s) \quad (18)$$

where L(s) is an arbitrary polynomial. Thus, assume Gp1(s) Gp2(s) and Gz1(s) Gz2(s) are coprime, and according to (24), choose Hz(s) and Hp(s) to satisfy:

$$G_2^P(s)H^P(s)G_1^P(s) + G_2^z(s)H^z(s)G_1^z(s) = G_2^P(s)H_1^P(s)G_1^z(s)L^*(s) \quad (19)$$

Then (22) become:

$$ACE_i(s) = \frac{s}{L^*(s)}\varepsilon(s) \quad (20)$$

Therefore, the performance of the ACE is determined by the polynomial $L^*(s)$. We can use a polynomial inverse to evaluate the LFC performance. However, it is difficult to obtain the analytical solution of (25), and $L^*(s)$ is a polynomial with multiple zeros, making performance analysis complicated. Fortunately, according to circuit theory, if open loop transfer function satisfies:

$$|G_2(s)H(s)G_1(s)| \gg 1 \quad (21)$$

the plant is in deeply negative feedback mode, then (21) can be simplified as:

$$ACE_i(s) \approx \frac{1}{G_2(s)H(s)}\varepsilon(s) \quad (22)$$

$G2(s)$ is determined by the system characteristics, so define disturbanceε':

$$\varepsilon'(s) = \frac{1}{G_2(s)}\varepsilon(s) \quad (23)$$

And then,

$$\frac{ACE_i(s)}{\varepsilon'(s)} \approx \frac{1}{H(s)} \quad (24)$$

And because, the numerator of $G2(s)$ is less than or equal to the denominator, so (29) can be expressed as:

$$\varepsilon'(s) = \left(\beta_{P-z}s^{P-z} + \beta_{P-z-1}s^{P-z-1} + \ldots + \beta_o + \frac{G_2'^P(s)}{G_2^z(s)}\right) \quad (25)$$

Hence, according to the superposition principle, (25) is the response of the superposition of the disturbance and its derivative, so it can be used to evaluate the dynamic characteristics of the ACE. Eq. (30) reveals that the ACE convergence properties are determined by the controller inverse. As a result, the LFC is transformed into the design of controller inverse. The controller design therefore becomes to look for its inverse to minimize the overshoot and settling time of its inverse step response.

2.5. Controller design based on controller inverse

Let the inverse form of controller be:

$$H(s)^{-1} = \frac{s(1+\alpha_1 s+\ldots+\alpha_{nb}s^{nb})}{K(1+\beta_1 s+\ldots+\beta_{na}s^{nb})} \quad (26)$$

Here, na and nb + 1 are numerator and denominator degree of controller, respectively. K is the gain. Its coefficient needs to be optimized. Particle swarm optimization (PSO) algorithm is a meta-heuristic algorithm based on swarm velocity and position, and widely used because they are simple and have the ability to obtain global optimum with a faster execution speed. Thus, PSO algorithm is used to obtain the parameters of controller. In the iterative process, the particle updates its velocity and position according to the individual and population optimal solutions. Then, let particle be ψ = [k, $\alpha 1$, …, αna, $\beta 1$, …, βnb], particle updated by:

$$V_j(n+1) = wV_j(n) + c_1r_1\left(\Psi_{best} - \Psi_j(n)\right) + c_2r_2\left(\Psi_{gbest} - \Psi_j(n)\right) \quad (27)$$

$$\Psi_j(n+1) = \Psi_j(n) + V_j(n+1) \quad (28)$$

$$w = w_{\max} - \frac{w_{\max}-w_{\min}}{n_{\max}} \quad (29)$$

where ψbest and ψgbest are individual and population optimal solutions, j is the particle index in the swarm, V is the velocity of particle, $c1$ and $c2$ are the cognitive and social acceleration factors, respectively; $r1$ and $r2$ are the random numbers uniformly distributed in the range [0,1], w is the inertia weight factor. The individual and total group optimization is determined according to the fitness function, and the fitness function defined as:

$Fmin = \gamma 1 max(Hstep) + \gamma 2 ts$

Here, Hstep is the step response sequence of (26), $\gamma 1$ and $\gamma 2$ are weight factor, respectively, ts is settling time. To ensure the solution quality, after the feasible solution is obtained by using PSO, continue to optimize and compare with the feasible solution, and retain the better solution until the solution remains unchanged.

3. Proposed Teaching Learning Based Optimization (TLBO) algorithm for proposed multi–Area System

The Teaching-Learning-Based Optimization (TLBO) algorithm, introduced by Rao et al., is a population-based metaheuristic optimization technique inspired by the teaching and learning process in a classroom. Due to its simplicity, fast convergence, and minimal parameter dependency, TLBO has become a powerful tool widely applied in various engineering optimization problems.

The TLBO algorithm operates in two main phases:

1. Teacher Phase – learning from the teacher (best solution)
2. Learner Phase – learning through interaction among learners

3.1 Initialization

In the initialization step, a population of candidate solutions is randomly generated. The population size is represented by NP, and the dimension of the problem is represented by D.

- NP: Number of learners (population size)
- D: Number of design variables (subjects)

The initial population matrix is defined as:

$$\boldsymbol{X} = \begin{bmatrix} x_{11} & x_{12} & \cdots & x_{1D} \\ x_{21} & x_{22} & \cdots & x_{2D} \\ \vdots & \vdots & \ddots & \vdots \\ x_{NP,1} & x_{NP,2} & \cdots & x_{NP,D} \end{bmatrix} \quad (30)$$

Each row represents a learner, and each column represents a subject (design variable). In the context of PID controller tuning, these variables correspond to controller parameters such as Kp, Ki, and Kd.

3.2 Teacher Phase

In the teacher phase, the best solution in the population is considered as the teacher, and the rest of the population represents learners. The objective of this phase is to improve the overall mean performance of the class.

First, the mean value of each design variable is calculated:

$$M_d = [m_1, m_2, \ldots m_D] \quad (31)$$

The difference between the teacher and the mean is computed as:

$$M_{diff} = r \cdot (X_{best} - T_F \cdot M_d) \quad (32)$$

where:

- r = random number in the range (0,1)
- Xbest = best solution (teacher)
- TF = teaching factor

The teaching factor is defined as:

$$T_F = round\big(1 + rand(0,1)\big) \quad (33)$$

Thus, TF takes either 1 or 2.

The population is then updated using:

$$X_{new} = X + M_{diff} \quad (34)$$

The updated solution is accepted if it improves the objective function:

$$f(X_{new}) < f(X) \quad (35)$$

This phase ensures that learners move toward better solutions guided by the teacher.

3.3 Learner Phase

In the learner phase, learners improve their knowledge by interacting with each other. Two learners are randomly selected, and their performance is compared.

If learner Xi is better than Xj, then:

$$X_i^{new} = X_i + r\big(x_i - x_j\big) \quad (36)$$

Otherwise:

$$X_i^{new} = X_i + r\big(x_j - x_i\big) \quad (37)$$

where rrr is a random number between 0 and 1.

The updated solution is accepted if it yields better fitness. This phase enhances diversity and avoids local minima.

4. Implementation of TLBO for PID Controller

The proposed TLBO algorithm is implemented in a MATLAB/Simulink environment to optimize PID controller parameters for Load Frequency Control.

- Simulation is performed for a multi-area interconnected power system
- A 5% step load disturbance is applied in area-1
- The objective function (typically ITAE – Integral of Time-weighted Absolute Error) is minimized

Simulation Parameters:

- Population size: NP=50
- Maximum iterations: 100
- Number of runs: 50

The best solution among multiple runs is selected as the final optimized controller parameters.

5. Performance Analysis

The performance of the proposed TLBO-tuned PID controller is evaluated and compared with other conventional and optimization-based methods such as:

- Ziegler-Nichols (ZN)
- Genetic Algorithm (GA)
- Bacterial Foraging Optimization Algorithm (BFOA)
- Firefly Algorithm (FA)
- Hybrid FA-PS

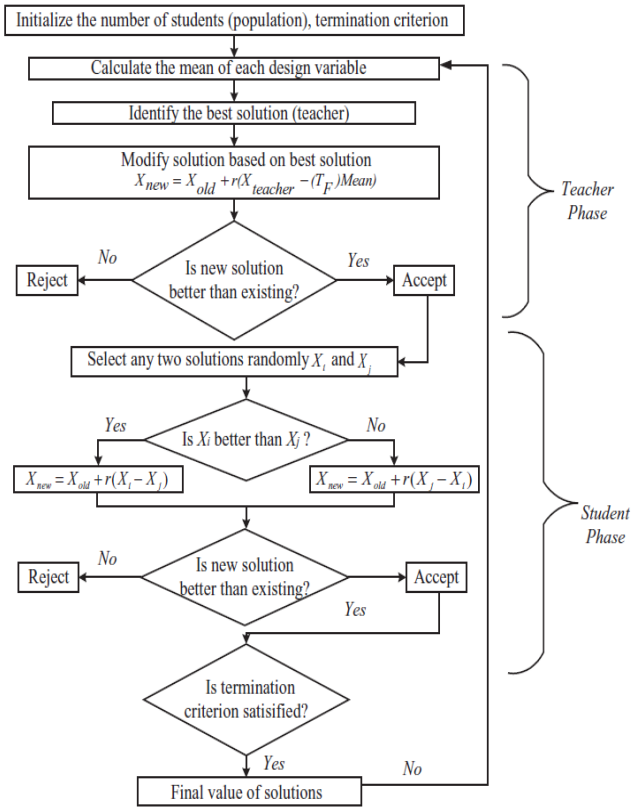

Fig. 2. The flow chart of TLBO algorithm

6. Simulation Results and Discussion

The effectiveness of the proposed TLBO-optimized PID controller for Automatic Generation Control (AGC) is evaluated under load disturbance conditions in an interconnected power system. The controller is designed to minimize frequency deviations and tie-line power oscillations while ensuring rapid system recovery. The dynamic responses of system frequency and tie-line power are shown in Fig. X(a) and Fig. X(b), respectively.

A. Frequency Response Analysis

Fig. 3 illustrates the frequency response of the interconnected power system controlled by the TLBO-optimized PID controller. Following the disturbance, the system experiences a very small frequency deviation from the nominal value of 50 Hz. A slight undershoot is observed initially, followed by a small overshoot before the frequency quickly settles to its steady-state value. The oscillations are highly damped and disappear within a few seconds, indicating excellent dynamic performance. The rapid restoration of frequency demonstrates the ability of the TLBO algorithm to determine optimal PID parameters that effectively improve damping characteristics and disturbance rejection capability.

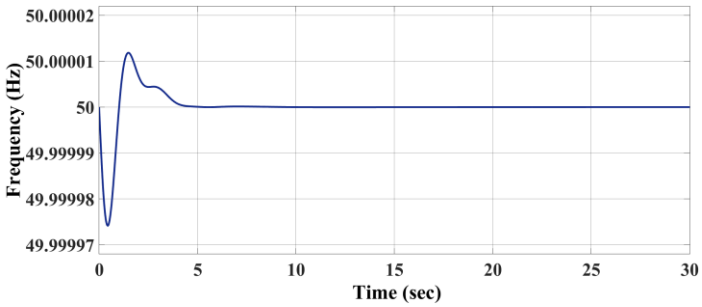

Fig.3 Frequency Stabilization Performance of the TLBO-Optimized PID Controller

B. Tie-Line Power Response Analysis

The tie-line power deviation response is presented in Fig.4. Immediately after the disturbance, a small transient deviation occurs in the tie-line power exchange between interconnected areas. However, the deviation decreases rapidly and converges to zero without sustained oscillations. The fast damping of tie-line power fluctuations indicates effective coordination between interconnected control areas and confirms the capability of the TLBO-optimized PID controller to maintain scheduled power interchange during system disturbances.

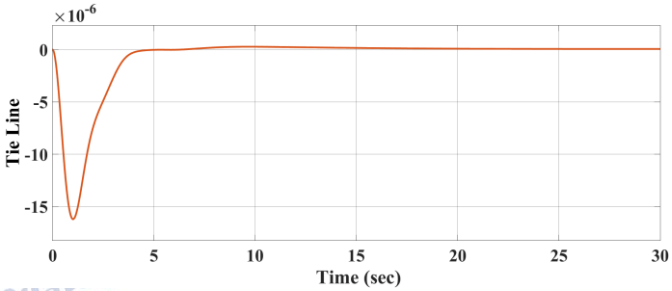

Fig.4 Tie-Line Power Regulation Performance of the TLBO-Optimized PID Controller

To evaluate the effectiveness of the proposed TLBO-optimized PID controller, its performance is compared with conventional PID and ANN-based controllers under the same disturbance conditions. The comparison is carried out in terms of system frequency deviation and tie-line power response, as shown in Fig. 5 and Fig. 6, respectively.

A. Frequency Response Comparison

Fig. 5 presents the frequency response of the interconnected power system for PID, ANN, and TLBO-based controllers. It can be observed that the conventional PID controller exhibits larger oscillations and a longer settling time following the disturbance. The

ANN controller improves the response by reducing oscillations and enhancing damping characteristics. However, the proposed TLBO-optimized PID controller provides the best performance, with minimal overshoot, reduced undershoot, and the fastest settling time. The frequency quickly returns to its nominal value of 50 Hz with negligible oscillations, demonstrating superior frequency regulation capability.

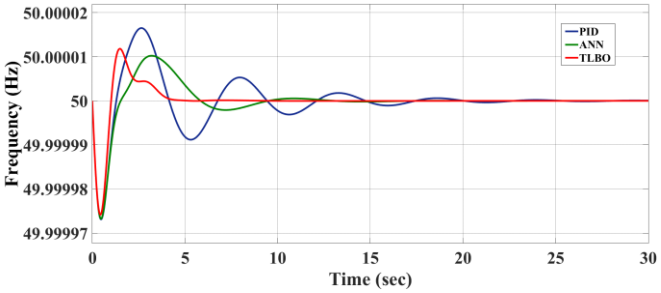

Fig.5 System Frequency Deviation Response under PID, ANN, and TLBO Control

B. Tie-Line Power Response Comparison

The tie-line power deviation responses are shown in Fig. 6. The conventional PID controller produces significant oscillations and requires a longer duration to restore the tie-line power to its steady-state value. Although the ANN controller improves the damping performance, noticeable transient deviations still exist. In contrast, the TLBO-optimized PID controller effectively suppresses tie-line power oscillations and rapidly drives the deviation to zero. This indicates improved coordination between interconnected areas and better control of power exchange following disturbances.

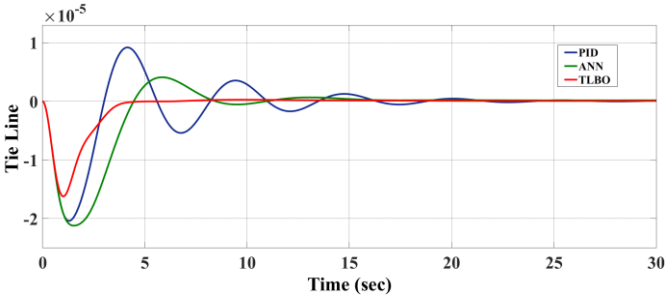

Fig.6 Tie-Line Power Deviation Comparison of PID, ANN, and TLBO Controllers

The simulation results clearly demonstrate the superiority of the proposed TLBO-optimized PID controller over both PID and ANN controllers. The optimized controller achieves faster frequency restoration, lower overshoot, improved damping characteristics, and reduced tie-line power fluctuations. These improvements are attributed to the effective parameter tuning capability of the Teaching-Learning-Based Optimization algorithm, which identifies optimal PID gains for varying operating conditions. Consequently, the proposed TLBO-based PID controller enhances frequency stability, improves dynamic performance, and ensures reliable operation of interconnected power systems with hybrid generation sources.

7. Conclusion

This paper presented a Teaching–Learning-Based Optimization (TLBO) tuned PID controller for frequency stabilization of interconnected power systems incorporating hybrid generation sources. The proposed controller was developed within the Automatic Generation Control (AGC) framework to effectively regulate system frequency and tie-line power deviations under varying load conditions and disturbances. By utilizing the TLBO algorithm, the PID parameters were optimally tuned to achieve improved dynamic performance and enhanced system stability. Simulation results demonstrated that the proposed TLBO-optimized PID controller effectively minimizes frequency deviations, suppresses oscillations, and significantly reduces settling time following load disturbances. The controller also provides superior tie-line power regulation, ensuring stable power exchange between interconnected areas. Comparative analysis with conventional PID and ANN-based controllers revealed that the TLBO-based approach offers faster response, improved damping characteristics, lower overshoot, and better disturbance rejection capability. Furthermore, the parameter-free nature and fast convergence characteristics of the TLBO algorithm simplify the optimization process while maintaining high-quality control performance. The obtained results confirm that the proposed controller enhances frequency stability and overall reliability of interconnected power systems with hybrid generation resources. Therefore, the TLBO-optimized PID controller represents an effective, robust, and computationally efficient solution for modern AGC applications in large-scale interconnected power networks.

Conflict of interest statement

Authors declare that they do not have any conflict of interest.

REFERENCES

[1] E. Papadis, G. Tsatsaronis, Challenges in the decarbonization of the energy sector, Energy 205 (2020) 118025.

[2] G. Zhang, F. Li, S. Wang, C. Yin, Robust low-carbon energy and reserve scheduling considering operational risk and flexibility improvement, Energy 284 (2023) 129332.

[3] G. Magdy, G. Shabib, A.A. Elbaset, Y. Mitani, Renewable power systems dynamic security using a new coordination of frequency control strategy based on virtual synchronous generator and digital frequency protection, Int. J. Electr. Power Energy Syst. 109 (2019) 351–368.

[4] K. Liao, Y. Xu, A robust load frequency control scheme for power systems based on second-order sliding mode and extended disturbance observer, IEEE Trans. Ind. Inform. 14 (2018) 3076–3086.

[5] K. Emami, T. Fernando, H.H.C. Iu, B.D. Nener, K.P. Wong, Application of unscented transform in frequency control of a complex power system using noisy PMU data, IEEE Trans. Ind. Inform. 12 (2016) 853–863.

[6] X. Shang-Guan, Y. He, C. Zhang, L. Jiang, J.W. Spencer, M. Wu, Sampled-data based discrete and fast load frequency control for power systems with wind power, Appl. Energy 259 (2020) 114202.

[7] R.P. Borase, D.K. Maghade, S.Y. Sondkar, S.N. Pawar, A review of PID control, tuning methods and applications, Int. J. Dynam. Control 9 (2021) 818–827.

[8] W. Tan, Tuning of PID load frequency controller for power systems, Energy Convers. Manag. 50 (2009) 1465–1472.

[9] G. Chen, Z. Li, Z. Zhang, S. Li, An improved ACO algorithm optimized fuzzy PID controller for load frequency control in multi area interconnected power systems, IEEE Access 8 (2020) 6429–6447.

[10] B.P. Sahoo, S. Panda, Improved grey wolf optimization technique for fuzzy aided PID controller design for power system frequency control, Sustain. Energy Grids 16 (2018) 278–299.

[11] R.K. Sahu, S. Panda, G.T.C. Sekhar, A novel hybrid PSO-PS optimized fuzzy PI controller for AGC in multi area interconnected power systems, Int. J. Electr. Power Energy Syst. 64 (2015) 880–893.

[12] D. Revathi, G.M. Kumar, Analysis of LFC in PV-thermal-thermal interconnected power system using fuzzy gain scheduling, Int. Trans. Electr. Energy 30 (2020).

[13] J. Liu, Q. Yao, Y. Hu, Model predictive control for load frequency of hybrid power system with wind power and thermal power, Energy 172 (2019) 555–565.

[14] D. Xu, J. Liu, X. Yan, W. Yan, A novel adaptive neural network constrained control for a multi-area interconnected power system with hybrid energy storage, IEEE Trans. Ind. Electron. 65 (2018) 6625–6634.

[15] Y. Mi, Y. Fu, C. Wang, P. Wang, Decentralized sliding mode load frequency control for multi-area power systems, IEEE Trans. Power Syst. 28 (2013) 4301–4309.

[16] F. Liu, Y. Li, Y. Cao, J. She, M. Wu, A two-layer active disturbance rejection controller design for load frequency control of interconnected power system, IEEE Trans. Power Syst. 31 (2016) 3320–3321.

[17] H. Li, X. Wang, J. Xiao, Adaptive event-triggered load frequency control for interconnected microgrids by observer-based sliding mode control, IEEE Access 7 (2019) 68271–68280.

[18] Z. Yan, Y. Xu, A multi-agent deep reinforcement learning method for cooperative load frequency control of a multi-area power system, IEEE Trans. Power Syst. 35 (2020) 4599–4608.

[19] L. Xi, L. Zhou, Y. Xu, X. Chen, A multi-step unified reinforcement learning method for automatic generation control in multi-area interconnected power grid, IEEE Trans. Sustain. Energy 12 (2021) 1406–1415.

[20] L. Yin, T. Yu, L. Zhou, Design of a novel smart generation controller based on deep Q learning for large-scale interconnected power system, J. Energy Eng. 144 (2018).

[21] C. Li, C. Feng, J. Li, D. Hu, X. Zhu, Comprehensive frequency regulation control strategy of thermal power generating unit and ESS considering flexible load simultaneously participating in AGC, J. Energy Storage 58 (2023) 106394.

[22] F. Ullah, X. Zhang, M. Khan, M.S. Mastoi, H.M. Munir, A. Flah, Y. Said, A comprehensive review of wind power integration and energy storage technologies for modern grid frequency regulation, Heliyon 10 (2024) e30466.

[23] M.W. Siti, N.T. Mbungu, D.H. Tungadio, B.B. Banza, L. Ngoma, Application of load frequency control method to a multi-microgrid with energy storage system, J. Energy Storage 52 (2022) 104629.

[24] F. Zhu, X. Zhou, Y. Zhang, D. Xu, J. Fu, A load frequency control strategy based on disturbance reconstruction for multi-area interconnected power system with hybrid energy storage system, Energy Rep. 7 (2021) 8849–8857.

[25] Y. Xu, C. Li, Z. Wang, N. Zhang, B. Peng, Load frequency control of a novel renewable energy integrated micro-grid containing pumped hydro power energy storage, IEEE Access 6 (2018) 29067–29077.